International Journal of Mechanical and Production Engineering Research and Development (IJMPERD)
ISSN (P): 2249-6890; ISSN (E): 2249-8001
Vol. 8, Issue 1, Feb 2018, 1255-1270

DESIGN, ANALYSIS AND FABRICATION OF SOLAR PV POWERED BLDC HUB MOTOR DRIVEN ELECTRIC CAR

M. PREMKUMAR[1], JSV. SIVAKUMAR[2], R. VIJAYA KRISHNA[3] & R. SOWMYA[4]

[1, 2, 3]*Assistant Professor, Department of EEE, GMR Institute of Technology, Rajam, Andhra Pradesh, India*

[4]*Research Scholar, Department of EEE, National Institute of Technology, Tiruchirapalli, Tamil Nadu, India*

ABSTRACT

Road transport has been dominated by petrol and diesel engines historically. Due to the environmental impacts and limited resources, both alternatives are unsustainable. The renewable energy directive, particularly identified as technology innovation, energy efficiency and renewable energy sources in the transport sector and it is considered as one of the most effective tools in reaching the targets in terms of sustainability and security of the supply. In this context, it is obvious that reaching the challenges depend on the rollout of Electric Vehicles (EV) as a sustainable transport and higher penetration of renewable energy sources. Here, a commercially marketable and simply designed electrical solar vehicle can replace fuel vehicles, controlling pollution and promoting wellness of the environment. It also creates awareness about the solar panel's future possibility and feasibility. Each part of the vehicle is designed and analyzed. This paper covers broad view on design and fabrication of a commercial renewable energy solar vehicle considering all the parameters within the limitations.

KEYWORDS: Renewable Energy, Electric Vehicle, Solar PV, Sustainability, Zero-Emission & Solar Race

Received: Dec 30, 2017; **Accepted:** Jan 20, 2018; **Published:** Feb 13, 2018; **Paper Id.:** IJMPERDFEB2018146

Original Article

1. INTRODUCTION

Today's transportation sector accounts for 23% of CO2 emissions, 72% of which is being emitted by road transport. The CO2 emission regulation for new cars has come as a response to set emission performance limits for new passenger cars with the goal of establishing a road map change for automotive sector. One significant challenge will consist in accommodating cost efficient fashion through active involvement of customer and better flexibility of the demand [1].

Many researchers are jointly working on future energy challenges, both in terms of security and sustainability, in that achieving a sustainable transportation system will be the critical component. Electrification of the transportation system seems to be the most promising alternatives in terms of increasing the security of supply and promoting a sustainable transportation through less pollutant resulting from conventional transportation [2], [4].

However, the care should be taken to the primary energy source, in fact the emissions generated by petrol/diesel engines could be counterbalanced by emissions generated from power plants. Further, centralized power source will result in high transmission losses and less efficiency. EV deployment may be considered as sustainable emission only when powered by the considerable amount of Renewable Energy Sources (RES). From power supply point of view, there is a limitation of accommodating an increasing level of RES sources under load demand from EV users both at peak and off peak time. On the other hand, an efficient penetration of RES depends on the ability to inject the maximum power within the stability of the electricity networks. Many studies had acknowledged and investigated

the EV potential in demand side management enhancement [6].

A zero-emission vehicle is powered by Solar energy by means of solar PV panels through storage batteries, and the traction is obtained by an electric motor. But, solar energy for EV is not an issue, because several critical points also need to be analyzed [7]. For example, the efficiency and costs of solar PV panels, how to maximize the solar irradiation, and the control and energy management. Nowadays, there are many researchers developing solar vehicle around the world for various purposes. From the research point of view, interesting contributions have been presented by researchers in two years like solar PV powered, zero-emission electric vehicle and solar/wind powered hybrid EV, with an internal combustion engine was proposed. A hybrid system for an EV is proposed, including solar PV, storage battery and super-capacitor, with the system configuration and different control strategy. The vehicle involving battery powered and charged by PV panels is used for agricultural activities in remote hilly areas, with the aim to produce the cleaner power hence the usage of diesel is reduced in agriculture. Other hand, many solar vehicles are built to participate in different solar vehicle championship around the world to test and examine the new technological advancements and its potential to design the zero-emission vehicles [3]. The design and development of electric solar vehicle is an initiative for students and researchers of various domains, motivated by solar vehicles race called "Electric Solar Vehicle Championship" in India.

The solar vehicle is another step to save the non-renewable sources of energy. The solar powered electric vehicle is also considered, because of less noise, less pollution and reduces greenhouse gas emission (GHG) emission. EV consists of PV panel, charger controller, battery, electronic speed controller and BLDC motor. The objective of the proposed design is, the energy drawn from the solar panel should be used to charge a battery which runs the motor of the vehicle. A simple DC-DC converter acts as interface between the solar panel and the battery to obtain the required constant voltage and it will extract maximum power from solar PV panel. Because of low maintenance, low weight, high efficiency, long life and compact design, BLDC motor is preferred over PMDC motor. This paper focuses on the design of solar PV, selection of battery and basic boost converter, mechanical structure and braking system for the solar vehicle driven by BLDC motor. The prototype solar vehicle is built and the vehicle is tested and verified. The rest of the paper is organized as follows: Section 2 focuses on the mechanical design of the vehicle. Section 3 deals with the electrical design of the vehicle. Section 4 discusses the experimental results. Finally, conclusions and future work are presented in Section 5.

2. Design and Testing of Mechanical Structure

2.1 Chassis Frame Structure

The frame of a vehicle is the skeleton. Safety for the driver and costly components such as panel and motor should be ensured from damage. The other main factor is weight reduction, which is a challenge to improve safety and stability with reduced weight. By considering the above factor, the frame is made up of AIS1020CR [9]. The skeleton is shown in figure 1.

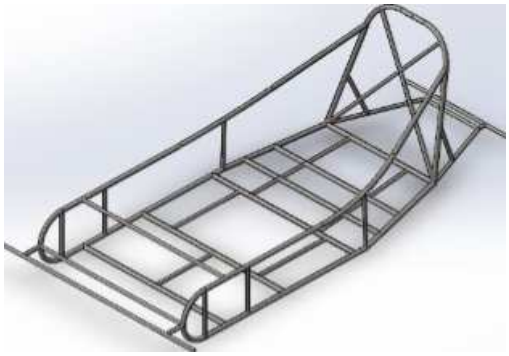

Figure 1: Basic Structure of the Vehicle Frame

The tests are carried out based on following procedure and parameters. Consider the vehicle hits an inelastic fixed object, for example, concrete wall. The four components of force are: magnitude, direction, point of application, and line of action Weight of Vehicle M: 180kgf (Driver weight = 60kgf), Speed of Vehicle v: 40km/hr = 12m/s, Time on impact t: 1/10th of a second.

Consider the total mass of vehicle as a single unit. The impact force is determined by using equation 1 and mass might be calculated according to equation 2.

$$F = \text{Mass (M)} * \text{Acceleration (a)} \tag{1}$$

$$\text{Mass} = {}^{\text{Weight}}/_{\text{Gravity}} = {}^{180}/_{9.81} = 21 \text{ kg} \tag{2}$$

The acceleration is calculated using equation 3 and the impact force on the wall is also calculated,

$$\text{Acceleration} = (V_o - V_1)/t = (0 - 12)/0.1 = 120 \text{ m/S}^2 \text{ (Deacceleration)} \tag{3}$$

$$\textit{Impact Force } F = 21 * 120 = 2520 \textit{ N} \tag{4}$$

where, V_o is velocity after impact i.e. 0 m/s, V_1 is velocity before impact i.e. 40km/hr = 12m/S and t is the time on impact i.e. 0.1S. The impact force is 14 times the weight of the vehicle. For this calculated force, the frame is tested and it is shown in figure 2 and the parameters from testing are listed in table 1.

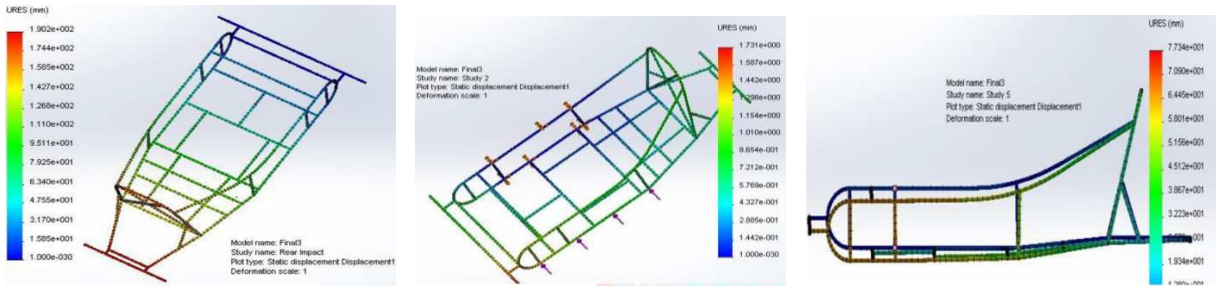

(a) **(b)** **(c)**

Figure 2: Frame Testing (a) Rear Impact; (b) Front Impact; (c) Front Impact

Table 1: Impact Test Parameters

Impact Test	Min. FOS	Max. Displacement (URES) In mm	Max. Stress Axial and Bending
FRONT	4.3	160	550 MPa

REAR	2.2	190	650 MPa
SIDE	5.4	1.731	140 MPa

Torsion test is conducted on the frame to determine the rigidity of the frame and ensures safety in real time. One side of the frame is fixed and load is applied on the other side. The simulation is done with load of 1000N. The result is expressed as Torsional stiffness, i.e. how much moment the frame requires to undergo 1^o of deflection and it is calculated as per equation 5.

$$K = M/\theta \tag{5}$$

where, M is moment in N-m and Θ is deflection angle. The moment is calculated by multiplying force and distance. For example, M = force*distance = 1000N * 1.016m = 1016N-m. The deflection angle is calculated from figure 3. The Torsional stiffness according to equation 5, K= 1016/4.39 = 232N-m/degree.

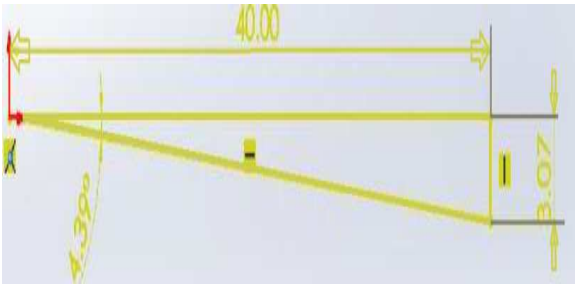

Figure 3: Calculation of Deflection Angle

Table 2: Torsional Test Parameters

Test	Front Torsion	Back Torsion	Full Torsion
Minimum FOS	2.8	2.34	2.4
Maximum displacement	76.79mm	40.37mm	77.34mm
Torsional Stiffness	210Nm/deg	254Nm/deg	232Nm/deg
Maximum Stress – Axial and Bending	240MPa	180MPa	235MPa
Maximum Stress - Torsion	160MPa	90MPa	140MPa

The static loading test is also conducted on the frame. Load carrying capacity of the vehicle is tested at the load of 1000N. Figure 4 shows the static loading test on the frame. For the load of 1000N, the minimum FOS is calculated as 2.1 and the maximum displacement of 13.84mm.

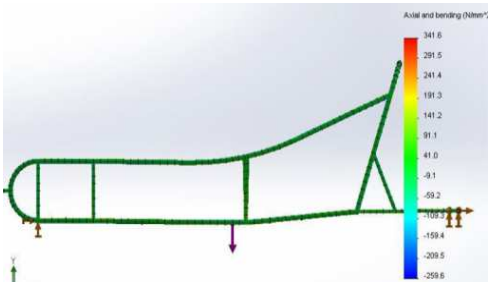

Figure 4: Static Loading Test at 1000N Load

Circular beam test is also conducted on the frame. The frame tube is heated and bent to a circular structure as shown in figure 5.

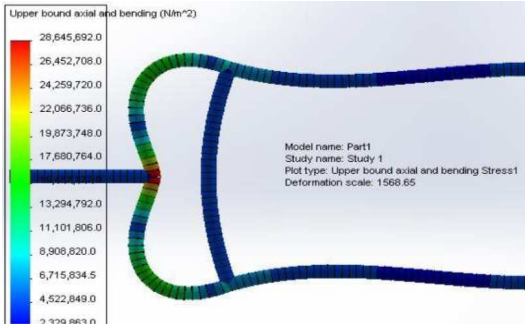

Figure 5: Upper Bound Axial and Bending at Deformation Scale of 1568.65

It is having advantage of load gets distributed evenly as there is no sharp curves and ability to bead more load and take in more stress before deformation. The comparison of circular beam and straight beam is listed in table 3.

Table 3: Comparison Study at Load of 250N

Parameters	Curved Beam	Straight Beam
Max. Stress N/mm^2	72	94
Min. FOS	12.2	8.4

From the comparison table, curved beam is preferred for the frame structure. The frame structures are bent inward to 1^o-2^o. This helps the beam to bend inward instead of bending outward. Bending outward can create cracks easily in the weld as it induce tensile stress. Curving inward induces compressive stress, which can be absorbed by a cross member.

2.2 Suspension System

When the vehicle is about to turn for certain degrees, the wheel on the inner side while turning experiences the maximum load than the outer side. This load might damage the wheels, frame etc. To avoid this or to minimize this, the suspensions are used. They are mainly used to enhance the comfort of the passengers, but it also helps in reducing the direct load to the frame [10].

2.2.1 Front Suspension

Initially, the dimension for the front track width is selected as 65 inches and it will offer resistance to the overturning moment at the Center of Gravity due to the inertial force and at the tires due to lateral weight transfer. The wheel base decides the longitudinal weight transfer during braking and acceleration. Finally, we get to know about the packaging of the components in the vehicle. So, it is decided to keep a wheelbase of 71 inches. Tyre generates the cornering force necessary during the turns. Its selection will have an effect on the performance of the vehicle. Due to the availability and economic design, the front wheel is having non geared two wheeler tyre and rear wheel is having YO speed bike tyre. The average pressures of the tires are 25psi at the front and 35psi at the rear. By keeping the above constraints, the front suspension is selected as a double wishbone suspension system. The kinematic analysis of double wishbone suspension system is done as shown in figure 6 and the values obtained from diagrammatic representation of the wishbones is shown in table 4.

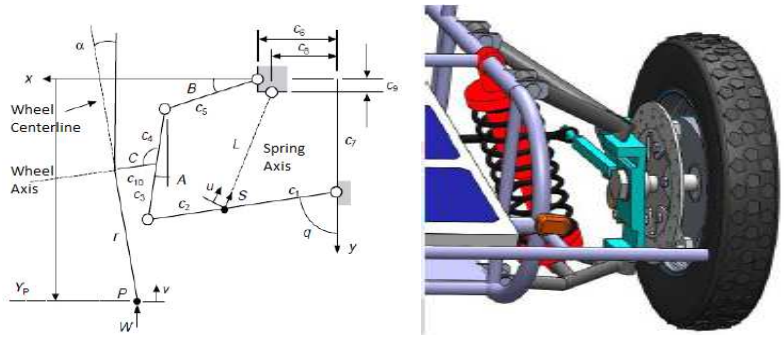

(a) (b)

Figure 6: (a) Analysis of Double Wishbone Suspension; (b) Front Suspension System

Table 4: Kinematic Analysis

For Dive	Chang E in Angle A	Chang E in Angle B	Chang E in Angle C	Chang E in Angle Q	Variation in Length L
-1	7	7.5	88	80	14
-0.7	10	13.5	88	85	13.6
-0.2	12	21	88	90	12.9
0.1 5	14	30	88	95	12.6
0.7	16	41	88	100	11.9

The roll centre is placed below the ground level with a value of -5.31 inches. The reason for negative value of the roll centre is that during cornering the rolling force is very minimal when the roll centre is negative. The approximate density of light mineral oil $_{\varrho}$, is 860 kg/m³. The thermal expansion of the fluid is, at T= 40°C, $_{\varrho}$=851.4 kg/m³, at T= 50°C, $_{\varrho}$=842.8 kg/m³, at T= 60°C, $_{\varrho}$=834.2 kg/m³. The compressibility of the suspension is, at P= 5MPa, $_{\varrho}$= 862.82 kg/m³, at P= 6MPa, $_{\varrho}$= 863.39 kg/m^3, at P= 7MPa, $_{\varrho}$= 863.97 kg/m³. The approximate viscosity of the fluid is 40.

2.2.2 Rear Suspension

The rear suspension is designed with oil damper suspension and it is shown in figure 7 (a). With a mono-shock rear suspension, a single shock absorber connects the rear swing arm to the motorcycle's frame. Typically this lone shock absorber is in front of the rear wheel, and uses a linkage to connect to the swing arm. Such linkages are frequently designed to give a rising rate of damping for the rear. The spring rate calculation is presented with known input parameters and it shown in figure 7 (b)-(c).

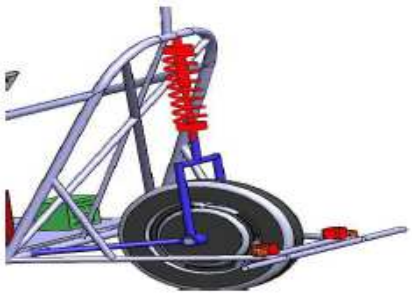

INPUT PARAMETERS	
Total Riding Weight (lbs)	441
Rear Weight Bias (%)	40
Rear Wheel Travel (in)	3.54
Shock Stroke (in)	4.92
Shock Sag (%)	25
Preload Adjuster (n.n)	14
End Coil Effect (%)	60

(a) (b)

Output Parameters	
Leverage Ratio (Travel/Stroke)	0.71
Calculated Spring Rate (lbs/in)	103
Suggested Spring Rate (lbs/in)	100
Suggested Spring Rate Preloaded Sag (%)	19.0

(c)

Optional Spring Rates		
Spring Rate (lbs)	Shock Sag (%)	Shock Sag (in)
-100	0-19.0	-0.93
-50	0-38.1	-1.87
0	na	na
50	19	1.87
*** 100 ***	*** 19.0 ***	*** 0.93 ***

(d)

Figure 7: (a) Rear Mono-Shock Suspension System; (b) Input Parameter for Spring Rate Calculation; (c) Output Parameters of Spring Rate Calculation; (d) Optional Spring Rates

2.3 Steering System

By taking less weight and steering ratio into consideration, the vehicle is designed with a steering system called Pitman Arm steering. The selection of steering system based on various parameters and it is listed in table 5.

Table 5: Selection Parameters for Steering System

Parameter	Pitman Arm	Rack And Pinion
Complexity	Fewer complexes. Can be easily machined.	More complex than pitman arm. System of gears is used.
Durability	Contacting surfaces are less which leads to high durability.	More wear and tear takes place due to gears.
Vibration	Vibration is less.	More vibration is transferred
Weight	Less weight compared to other steering systems.	More weight.
Turning Sensitivity	Quick turns can be achieved in sharp corners since the steering ratio used is 1:1- 1:2	During turning 3 to 4 complete revolutions are required from lock to lock.

The steering ratio is a ratio between the steering wheel turning angle to the wheel turning angle. The steering ratio of 1:1.126 is selected for this vehicle. i.e., the wheel turning angle is same as that of the steering wheel. The circular arc formed by the turning path radius of the front outside tire of a vehicle is called turning radius r and it is selected as 240inches and it is shown in figure 8.

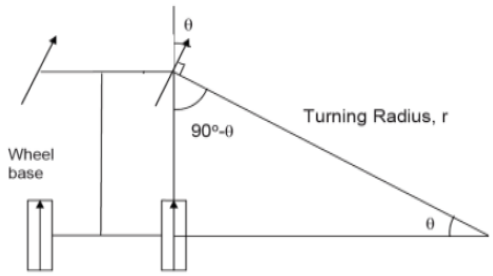

Figure 8: Turning Radius

The various parameters of steering parameters are selected by considering advantages and figure 9 will give a detailed explanation on steering parameters. The angle of the wheel with respect to the vertical axis from front view is called negative camber angle and it is selected as 2^0 and for the neutral camber, it is 0^0. Steering axis inclination / King pin inclination is 5^O with positive inclination, toe in angle of 1^0 Positive, max steering wheel angle is 90^0 for each side,

maximum turning angle is fixed as 71^0 and finally, King pin to wheel axle orientation is selected as neutral.

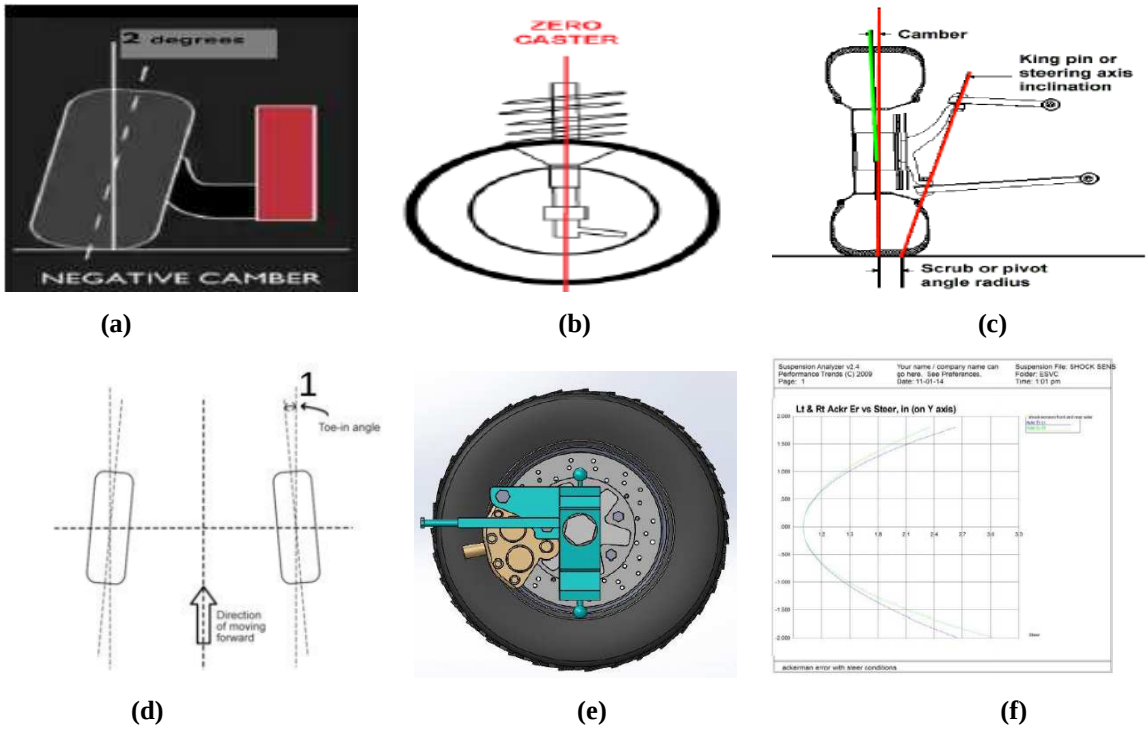

(a) **(b)** **(c)**

(d) **(e)** **(f)**

Figure 9: (a) Negative Camber; (b) Neutral Camber; (c) Steering Axis Inclination; (d) Toe Angle; (e) Wheel Axle Orientation; (f) Response form Suspension Analyzer

A good steering system must satisfy Ackerman condition. During turns slight variation is unavoidable. Large variation will lead to steering system failure. The figure 9 (f) shows the variation of Ackerman in the amount of steering. This was analyzed using suspension analyzer giving condition as steering. From figure 9(f), it is clear that the Ackerman variation/error is minimal under steering which represents a good steering system design. The steering system is fixed in vehicle as per the diagram shown in figure 10.

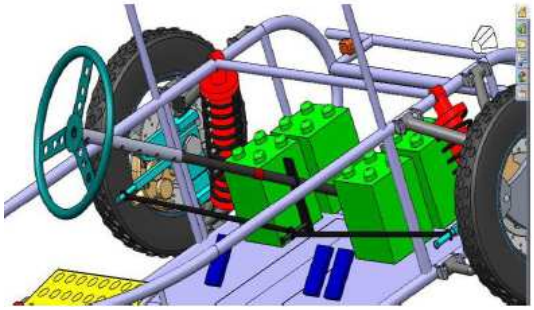

Figure 10: CAD Model of Steering System

2.4 Braking System

The brakes are one of the most important control components of the vehicle. They are required to stop the vehicle within the smallest possible distance and this is done by converting the kinetic energy of the vehicle into the heat energy which is dissipated into the atmosphere. In this vehicle, two disc brakes are used on the front axle to be more effective and drum brake on rear axle assisting to slow or stop the vehicle instantly after applying the brakes. Tandem master cylinder is used as a master cylinder in a vehicle, because the tandem master cylinder transforms applied brake force into hydraulic

pressure which is transferred to the wheel units through two separate circuits. This provides residual braking in the event of fluid loss.

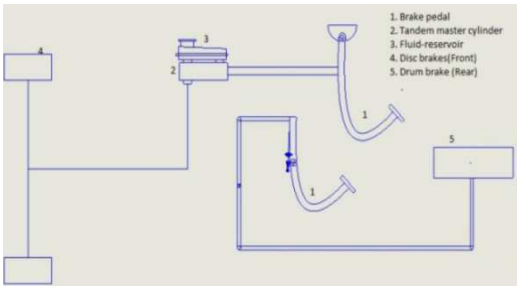

Figure 11: Braking Circuit

In braking circuit as shown in figure 11, the two independent lines from the tandem master cylinder are actuated by single pedal for locking the two wheels on front effectively. And also provide another one pedal for locking the rear wheel with drum brake. In a disc brake, the brake pads squeeze the rotor instead of the wheel, and the force is transmitted hydraulically instead of through a cable. Friction between the pads and disc slows the disc down. The parts are taken from various vehicle and table 6 shows the parts and their respective vehicle.

Table 6: The Various Parts of Braking System

Part Name	Qty.	Manufacturer
Tandem master cylinder	1	Maruti Omni
Disc (or) Rotor	2	Pulsar150 (Pearlitic Gray CI)
Caliper	2	Pulsar 150
Actuation Pedal	2	Maruti Omni Actuation pedal
Brake Lining	-	Maruti Omni brake hoses
Brake Fluid	-	Dot 3

By considering the various issues in designing a proper braking system, the various parameters are calculated with some design consideration. The table 7 shows the braking parameters and the braking efficiency of the vehicle is calculated as per equation 6.

Table 7: Braking Parameters

Sl. No	Parameters	Calculated Value
1	Pedal Ratio	6:1
2	Pedal Force	305.58 N
3	Fluid Pressure	5.29 * 106 N/m^2
4	Clamping Force	9606.64 N
5	Brake Force	4803.32 N
6	Braking Torque	432.3 N-m
7	Deceleration of the vehicle	19.92 m/s^2
8	Stopping Distance	2.37 m
9	Stopping Time	0.96 sec
10	Efficiency	65% (Fair)

$$\eta \text{ in } \% = {(\text{Total weight of the vehicle})}/{Brake\ Effort} * 100 = {200}/{305.58} * 100 = 65\%\ (Fair) \quad (6)$$

2.5 Ergonomics

Ergonomics refer to the design factors, as for the workplace, intended to maximize productivity by minimizing operator fatigue and discomfort. Vehicle is properly designed to give additional safety and comfort. Egress time depends on position of the driver. Driver's comfort depends on the position he sits. A good position can make a driver go long drives without any fatigue and stress and enjoy the drive. The position shown in 12(a), seat must provide comfort and shouldn't allow driver to slip in turns. If the weights must also lie close as possible to the CG point, so that vehicle spin with respect to vertical axis is used which gives additional advantage while steering by overcoming under steering. The figure 12(b) shows the concept of weight distribution affecting handling. The following problem arises when the placement of battery, 1. Placing inward – more vehicle spin; 2. Placing outward – more moment in turns. So the batteries are placed to balance out both these effects.

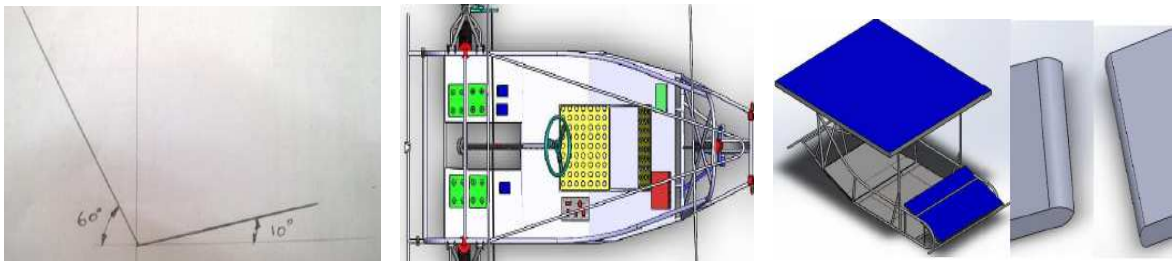

(a) **(b)** **(c)**

Figure 12: (a) Seating Position; (b) Weight Distribution; (c) Solar Panel Placement

In order to minimize the under-steering, the batteries are closed in near CG point. Space for the driver must also be considered. The solar panel placement is also crucial role and it is shown in figure 12(c). Totally 3 panels are used.2 panels are placed on top with 50inch high and one in front. Totally 50squarefeet of panels are used. Panels are placed with the following consideration: 1. Maximum sunlight reception; 2. Aerodynamics of the vehicle; 3. Convenience for the driver. The ends of solar Panel are made into curves with a thin gauge sheet metal to reduce air drag. The more weight on the forward wheels, the better the cornering and less over-steer. However, too much weight on the front wheel causes the rear wheel to wash-out during hard cornering or cause the trike to end-over during braking. Driver's visibility is restored to 220^0. Additionally, 2 rear view mirrors are provided to check the other 140^o is provided to 2 rear view mirrors on either side. Driver will have a clear visibility of 360^o.

3. DESIGN AND TESTING OF ELECTRICAL SYSTEMS

The overall block diagram of electrical system is shown in figure 13. The vehicle is powered with solar PV panel through MPPT charge controller to extract more power from the solar PV module and battery source. The motor is supplied with battery power and solar module power individually and it is controlled by changeover switch.

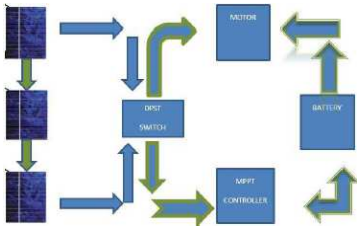

Figure 13: Flow Diagram of Electrical Systems

3.1 Solar Panel with MPPT Charge Controller

All over the world there is significant increase in usage of solar energy. Fuel replaced by Solar panel. All the automobile companies have their project works –going in solar power to run vehicles in solar energy. Based on the design of solar panel, the entire vehicle is designed because of it being the most dominating feature. The power rating of the motor is 700W. So, the solar PV is designed with 750W by keeping 50W as tolerance. The total number of PV panel used in this vehicle is 3 and each having 250W.

The specification of solar PV is as follows. Maximum voltage from one cell is 0.666V, the available size of 48V solar panel for all 3 panel is 49 Square feet, maximum voltage from one 72 cells of solar panel at open circuit is 59.5V, the maximum voltage output at average condition of sunlight is 48.5V, maximum current from one 72 cells of solar panel at open circuit is 8A, the maximum current output at average condition of sunlight an short circuit is 5.15A, the maximum power output from a solar panel at average condition of sunlight is 250Wand maximum power output from 3 solar panel output is 750W.

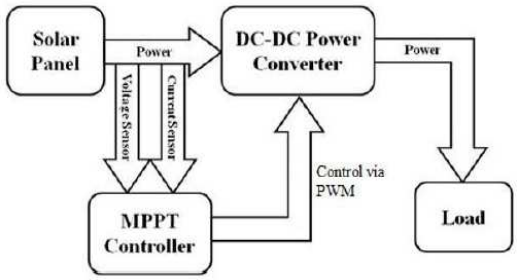

Figure 14: Block Diagram of Electrical Systems

A MPPT, or maximum power point tracker is an electronic DC to DC converter that optimizes the match between the solar array (PV panels), and the battery bank or utility grid and block diagram is shown in figure 14 [5], [13]. To put it simply, they convert a higher voltage DC output from solar panels (and a few wind generators) down to the lower voltage needed to charge batteries.

3.2 BLDC Hub Motor

The vehicle designed with 750W BLDC motor (brushless DC). BLDC motor is a type of synchronous motor, where magnetic fields generated by both stator and rotate have the same frequency. The BLDC motor has a longer life because no brushes are needed. Apart from that, it has a high starting torque, high no-load speed and small energy losses. Out of many configurations, three phase motors are the most popular and are widely used in e-bikes. The vehicle is selected with hub motor because the motor replaces the hub of wheel. Coupling loss is reduced and mounting can be made easy without the use of chains or belts, and that reduces size and weight of the car.

Figure 15: BLDC Hub Motor

Diameter of wheel is 10 inches and radius of the wheel is 0.127m is selected for a test drive. The various test on hub motor is conducted and test results are shown in table 8 and characteristics are shown in figure 16. The test is conducted with 200kg and 300kg load.

Table 8: No Load and Load Test Data on Hub Motor

Sl. No	Weight (kg)	Speed (Kmph)	Speed (rpm)	Load Current (A)
1	No Load	10	208.9	4.1
2		20	417.9	4.1
3		30	626.9	4.1
4		40	835.8	4.1
5	200	10	208.9	10
6		20	417.9	15
7		30	626.9	16
8		40	835.8	25
9	300	10	208.9	18.5
10		20	417.9	27.5
11		30	626.9	28.1
12		40	835.8	29.5

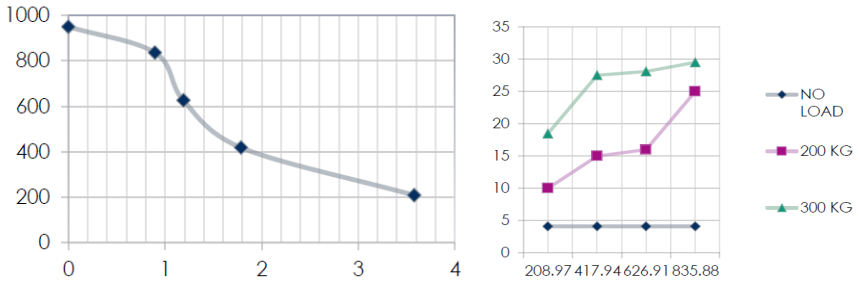

(a) **(b)**

Figure.16: Performance Characteristics, (a) Torque in Nm Vs Speed in rpm; (b) Speed in rpm Vs Load Current in A

3.3 Battery Unit with Charging Parameters

Battery based renewable energy systems vary greatly in size and design based on the purpose and location of the installation. Unlike many other battery applications, this battery based renewable energy applications are unique because the batteries can be discharged and then charged in a very unpredictable manner due to variations in sunshine. Deep cycle valve regulated Lead-Acid batteries (VRLA) or sealed battery is the best choice for renewable energy applications but it is also recognized that there are different types having strengths and weaknesses which influence their suitability and life [11]. This solar car utilizes lead acid battery and four lead-acid batteries will be connected in series to drive a hub motor through a controller. To maintain the stability of the car in the best possible way the batteries are split up into four and placed in the most comfortable region. The batteries are charged with 48V, 2.5A, charger circuit which is powered by solar panel (1000W).

The vehicle is designed with four 12V batteries which are connected in series; hence the input voltage should be 48Vat the minimum. Since the charging potential should be greater than battery potential we boost up the voltage level to 50Vor more. The minimum charging current should be 10% of rated battery current. So, the charging current for the battery is 3.3A. Considering the lifetime of battery, charging current is also boosted up to 3.5Aor more. The time taken for

the 33AH batteries to charge is 9.4 hours. However, it is impossible to charge the battery without any efficiency loss, hence the following table 9 shows the time taken to charge with efficiency loss. The time taken to discharge depends on the load current. The maximum current that the motor will draw under full load is 16.6A. So, the discharge time is 1.16 hours (on full load). The graph is shown in figure 17 is plotted to show the capacity of battery at the different charging interval at 27^{o}C temperature.

Table 9: Charging Time with Various Efficiency Loss

Maximum Time To Full Charge (10% Efficiency Loss)	10.3 Hours
Maximum Time To Full Charge (20% Efficiency Loss)	11.3 Hours
Maximum Time To Full Charge (30% Efficiency Loss)	12.4 Hours
Maximum Time To Full Charge (30% Efficiency Loss)	13.4 Hours
Maximum Time To Full Charge (No Efficiency Loss)	9.6 Hours

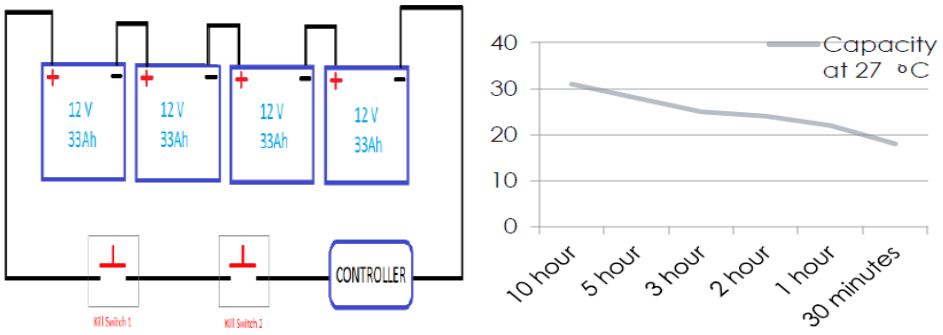

(a) **(b)**

Figure 17: (a) Battery Wiring Diagram; (b) Capacity of Battery with Different Charging Interval

3.4 Electronic Speed Control Unit of Hub Motor

A motor controller is a device or group of devices that serves to govern, in some predetermined manner, the performance of an electric motor. A motor controller might include a manual or automatic means of starting and stopping the motor, selecting forward or reverse rotation, selecting and regulating the speed, regulating the speed, regulating or limiting the torque, and protecting against overloads and faults. It is the brain of the vehicle and it is a multi-functioning device. On receiving battery voltage, it activates. It provides signal voltage to all major electronic components like accelerator, brake, motor, etc. and it uses Hall Effect sensors to direct the rotor's position [12]. The specification is shown in table 10.

Table 10: Specification of Electronic Speed Controller

Input	48 volts DC from battery
Output	AC 5 volts to the system.
Hall Sensor Type	60^{o} or 120^{o} (60^{o} is used here)
Electric Signal	AC Pulse
Type Of Output	5V SYSTEM (Overload indication, lights, hall censors)
Min. O/P Voltage	20 volts
Full Load Current	20 A

The controller for receiving the accelerator signal, the controller supplies power from battery to motor. Because the controller must direct the motor's rotor rotation, the controller needs some means of determining the rotor's position.

There by using Hall Effect sensors we will be able to directly measure the rotor's position. The controller contains 3 bi-directional drivers to drive high-current DC power, which are controlled by a logic circuit. Position information can be gotten by Hall Effect sensors that detect the rotor magnet position. By pressing the accelerator, the hall sensor mounted inside the accelerator sends signal to the controller. The controller sends power to the motor proportional to the pressing force of the accelerator. The speedometer shows indication proportional to the pressing force of the accelerator. Borax contains electronic sensors in the form of pedal. It receives signals from the controller. On applying the brake, the signal is sensed by the controller and controller stop sending power to the motor. It saves power when frequent braking situation arises. The speed control unit is shown in figure 18.

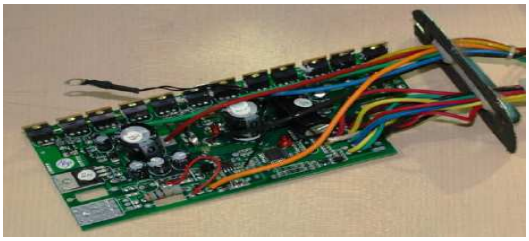

Figure 18: Interior View of Electronic Speed Controller

RESULTS AND DISCUSSIONS

The car requires more torque and acceleration. The hub motor develops maximum torque at low rpm, then torque decays with speed in steps with car natural demand. Solar power from solar PV is limited by the size of the car and area that can be exposed to sunlight. While energy can be accumulated in batteries to lower peak demand on the array and provide operation in sunless conditions. SEPHV is combined technology of solar and electric power. Solar vehicle depends on PV cells to convert sunlight into electricity to drive electric motors. The weight estimation of the proposed vehicle is listed in table 11 and chart is shown in figure 19.

Table 11: Weight Estimation of Proposed Car

Department	Weight(Kg)
Motor and Controller	11.5
Solar Panel and Charge Controller	51
Batteries and Accessories	29
Frame, Base & Weld	26
Steering System	2
Braking System	9.3
Ergonomics	6.15
Miscellaneous	11.5
Driver Weight	60
Overall Weight of Car	206.45

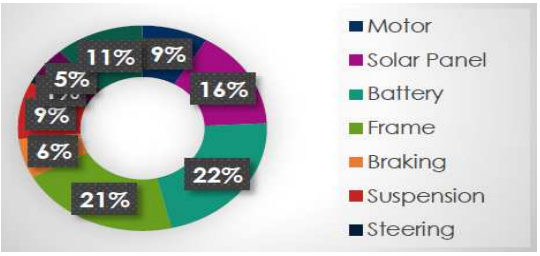

Figure 19: Weight Estimation Chart

Speed is controlled through accelerator pedal which is connected with electronic speed controller. Solar PV panel is mounted on top of the vehicle and it will charge the batteries via MPPT charge controller. Three 250W solar panels is used to charging the batteries and it will drive the motor with load nearly 250kg including the weight of driver. The maximum speed of the proposed car is limited 40kmph. The battery will be continuously gets charged by the solar panel. During less irradiance, the battery alone will drive the motor and it provides the continuous run for the vehicle. Figure 20(a) shows the proposed solar car solar vehicles race in India and figure 20(b) shows the battery placement with safety measures.

(a) **(b)**

Figure 20: (a) Assembled Electric Solar Car for Race; (b) Placement of Battery

The cost report is presented in figure 21 which will give details on how economically the car is designed and how the cost is distributed among each part of the vehicle. From the final observation, it is essential to notice the issue related with the appropriate utilization of solar power during the race. As showed in Figure 20(a), the top roof demonstrates an inclination of 40^{o} over horizontal axle by the solar tracking system.

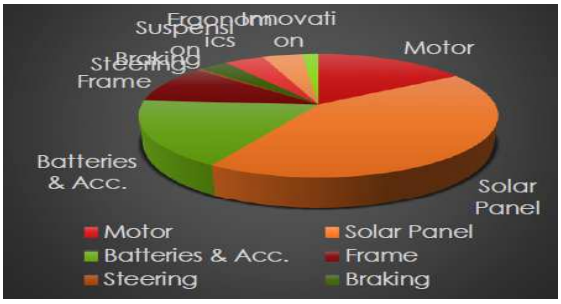

Figure 21: Cost Distribution

CONCLUSIONS

The importance of this proposed car is making the shift to the source of energy which is made cost effective, and utilization of solar power was implemented. The objective of selecting the suitable components was studied and analyzed. The various components for the same is subjected to various tests which was cross checked with simulation results. The main features of the proposed design of solar vehicle combine PV energy and human energy. Distinct importance has been strained to PV solar energy as main power source. The results related to chassis, transmission, suspension, braking, weight, and all electrical systems were obtained by conducting various test and with simulation tools. The overall cost of the solar PV is less than other solar PV modules. The research in different stages led to the utilization of lead-acid battery

because of its characteristics and for its use in electric car especially. Batteries were placed on the back side of the car and the electric motor is powered through the control circuit. The car can achieve a maximum speed of 45kmph for a distance of 100 km, depending on energy savings. The car travels without any noise and without any toxic gas emission, it is a friend of the environment. Conceivable enhancements for the electric vehicle will be planned in future work, taking into account the zero emission and the incorporating the new technologies as the main strategies.

REFERENCES

1. *E. J. Caims, "A new mandate for energy conversion: zero emission (electric) vehicles," In: Proc. of IEEE 35th International Power Sources Symposium, 1992, pp.310-313.*
2. *G. Maggeto and J. Van Mierlo, "Electric and electric hybrid vehicle technology: a survey," In: Proc. of IEE Seminar on Electric, Hybrid and Fuel Cell Vehicles, 2000, pp.1/1-11.*
3. *S. Matsumoto, "Advancement of hybrid vehicle technology," In Proc. of IEEE European Conference on Power Electronics and Applications, 2005, pp.1-7.*
4. *D. Gopalakrishnan, V. Gopu & V. Gopalakrishnan, Torque Ripple Minimization of BLDC Motor by Using Hysterisis Current Controller, International Journal of Electrical and Electronics Engineering Research (IJEER), Volume 5, Issue 2, March - April 2015, pp. 51-60*
5. *L. Situ, "Electric Vehicle Development: the past, present & future," In: Proc. of 3rdInternational Conference on Power Electronics Systems and Applications, 2009, pp.1-3.*
6. *L. Zhihao and A. Khaligh, "An integrated parallel synchronous rectifier and bi-directional DC/DC converter system for solar and wind powered hybrid electric vehicle," In: Proc. of IECON, 2009, pp.3779-3784.*
7. *Bin Wu, Fang Zhuo, Fei Long, WeiweiGu, Yang Qing, and YanQin Liu, "A management strategy for solar panel -battery-super capacitor hybrid energy system in solar car," In: Proc. of ICPE & ECCE, 2011, pp.1682-1687.*
8. *D. A. G. Redpath, D. McIlveen-Wright, T. Kattakayam, N. J. Hewitt, J. Karlowski, and U. Bardi, "Battery powered electric vehicles charged via solar photovoltaic arrays developed for light agricultural duties in remote hilly areas in the Southern Mediterranean region," Journal of Cleaner Production, vol.1, no.18, 2011, pp.2034-2048.*
9. *S. Vishnu et al., Design and Implementation of Zeta Micro-Inverter for Solar PV Application, International Journal of Mechanical and Production Engineering Research and Development (IJMPERD), Volume 7, Issue 4, July - August 2017, pp. 215-222*
10. *R. Mangu, K. Prayaga, B. Nadimpally, and S. Nicaise, "Design, development and optimization of highly efficient solar cars: GatoDel Sol I-IV," In: Proc. of IEEE Green Technology Conference, 2010, pp.1-6.*
11. *S. S. Wilson, 1973, Bicycle technology, Scientific American, 228(3), 81-91.*
12. *F. R. White and D. G. Wilson, Bicycle Science, 2nd ed., Ed. The MIT Press, 1982.*
13. *T. L. Gibson and N. A. Kelly, "Solar photovoltaic charging of lithium-ion batteries", Journal of Power Sources, vol.195, 2010, pp.3928-3932.*
14. *M. Premkumar, and R. Sowmya, "Regenerative electric braking on electric bicycle and storage of energy using ultra capacitor," Journal of Advanced Research in Dynamical and Control Systems, vol.11, no.16, 2017, 86-99.*
15. *M. Premkumar, N. Dhanasekar, R. Dhivakar, and P. Arunkumar, "Comparison of MPPT algorithms for PV systems based DC–DC converter," Advances in Natural and Applied Science, vol.17, no.9, 2015, pp.212-*